THE ASTROPHYSICAL JOURNAL, 557:L75–L78, 2001 August 10

DIAGNOSTIC UTILITY OF THE RELATIVE INTENSITY OF 3C TO 3D IN Fe XVII

G. V. BROWN,[1] P. BEIERSDORFER, H. CHEN, M. H. CHEN, AND K. J. REED
Physics and Advanced Technology, Lawrence Livermore National Laboratory, 7000 East Avenue, Livermore, CA 94551
Received 2001 March 15; accepted 2001 June 27; published 2001 July 26

ABSTRACT

The relative intensity R of the resonance and intercombination line in neon-like Fe XVII, located at 15.01 and 15.26 Å, respectively, has been measured at the Lawrence Livermore National Laboratory electron beam ion trap EBIT-II as a function of the relative abundance of sodium-like Fe XVI. Our measurements identify several Fe XVI lines and one Fe XV line in this region. We show that an Fe XVI inner shell satellite line coincides with the intercombination line and can significantly reduce the apparent R. We measure $R = 1.90 \pm 0.11$ when the relative abundance of Fe XVI to Fe XVII is ~1. This explains the anomalously low ratios observed in the solar and stellar coronae. The fact that the apparent relative intensity of the resonance and intercombination line in Fe XVII is sensitive to the strength of an Fe XVI inner shell satellite, and therefore, the relative abundance of Fe XVI to Fe XVII, makes the line ratio a diagnostic of temperature.

Subject headings: atomic data — line: identification — stars: coronae — Sun: corona — Sun: X-rays, gamma rays — X-rays: general

1. INTRODUCTION

The L-shell line emission spectrum of Fe XVII is observed over a large temperature range. It has been recorded and well resolved in the corona of the Sun (Rugge & McKenzie 1985; Phillips et al. 1982; Hutcheon, Pye, & Evans 1976; Parkinson 1975) and in extrasolar sources (Canizares et al. 2000; Brinkman et al. 2000). Two of the most distinct lines observed from Fe XVII are the $1s^2 2s^2 2p^5_{1/2} 3d_{3/2}\ ^1P_1 \rightarrow 1s^2 2s^2 2p^6\ ^1S_0$ resonance and $1s^2 2s^2 2p^5_{3/2} 3d_{5/2}\ ^3D_1 \rightarrow 1s^2 2s^2 2p^6\ ^1S_0$ intercombination lines at 15.01 and 15.26 Å known as 3C and 3D, respectively.

Values of the relative intensity of the two Fe XVII lines, $R = I_{3C}/I_{3D}$, between 1.6 and 2.8 have been measured from nonflaring active regions of the solar corona (Waljeski et al. 1994; McKenzie et al. 1980; Hutcheon et al. 1976; Parkinson 1975; Blake et al. 1965). Values in the range of 2.6–2.8 have been measured from Capella (Mewe et al. 2001; Brinkman et al. 2000). By contrast, measurements on the electron beam ion trap EBIT-II gave an average value of 3.04 ± 0.12 for electron impact-excitation (Brown et al. 1998). New measurements over a wide energy range have shown that this ratio, within a narrow range, is invariant to the type of excitation process, including radiative cascades, resonance excitation, and blends with unresolved dielectronic satellite lines (Brown, Beiersdorfer, & Widmann 2001; Brown 2000).

The EBIT-II value of 3.04 agrees only with some of the higher values measured from the Sun and is marginally in agreement with the Capella ratio. The question arises as to the cause of the lower ratios, and hypotheses have been put forth, including resonance scattering (Saba et al. 1999; Schmelz et al. 1997; Waljeski et al. 1994; Rugge & McKenzie 1985). In the following, we show that the low ratio is produced by coincidence of an Fe XVI line with that of 3D. The ratio, therefore, is sensitive to the relative abundance of Fe XVI and Fe XVII, making it a measure of the charge balance and thus of the electron temperature.

2. MEASUREMENT AND RESULTS

The present measurements were carried out as part of the laboratory astrophysics program at the Lawrence Livermore National Laboratory electron beam ion trap EBIT-II (Beiersdorfer et al. 2000a,[2] 2000b; Gu et al. 1999; Savin et al. 1996). In order to measure the effect of the Na-like Fe XVI inner shell (IS) satellites on the ratio R, it is necessary to have a significant amount of Fe XVI and Fe XVII ions present in the trap simultaneously at electron beam energies high enough to excite lines 3C and 3D in Fe XVII and IS satellites in Fe XVI, i.e., energies greater than ~830 eV. However, because the ionization energy of Na-like Fe XVI is only 489 eV, the ion population in a monoenergetic beam between 830 and 1200 eV is nearly 100% Fe XVII in equilibrium. Indeed, this was found when we used the metal vapor vacuum arc (MeVVA) to inject and study Fe XVII in our trap (Brown et al. 1998). Hence, in order to study the effects of Fe XVI IS satellites on the Fe XVII line emission, a way must be found to maintain a large fraction of Fe XVI. We resolved this issue by using EBIT-II's ballistic gas injector to continuously introduce neutral iron into the trap as iron pentacarbonyl, $Fe(CO)_5$. The introduction of a stream of neutrals results in an underionized plasma and thus a lower ionization balance. Moreover, the ionization balance can be regulated by the flow of neutrals into the trap, i.e., by the gas injector pressure. The relative abundance of Fe XVI to Fe XVII ions was between ~0.15 and ~1.0 at gas injector pressures between 1×10^{-7} and 1×10^{-6} torr.

The X-rays emitted from EBIT-II were measured using a flat crystal spectrometer (Brown, Beiersdorfer, & Widmann 1999) employing a rubidium acid phthalate (RAP) crystal for diffraction and a position sensitive proportional counter for detection. The resolving power of this spectrometer is $\lambda/\Delta\lambda \cong 575$ at 15 Å.

Figure 1 shows the spectra measured during this experiment. The spectrum in Figure 1*a* was measured at a high gas injection pressure, and the spectrum in Figure 1*b* was measured at a low gas injection pressure. Figure 1*c* shows a spectrum measured when iron was injected using a MeVVA after reaching ionization equilibrium. These spectra were measured using a mono-

[1] Currently an NRC associate at Goddard Space Flight Center; gvb@milkyway.gsfc.nasa.gov.

[2] See also http://heasarc.gsfc.nasa.gov/docs/heasarc/atomic/proceed.html.

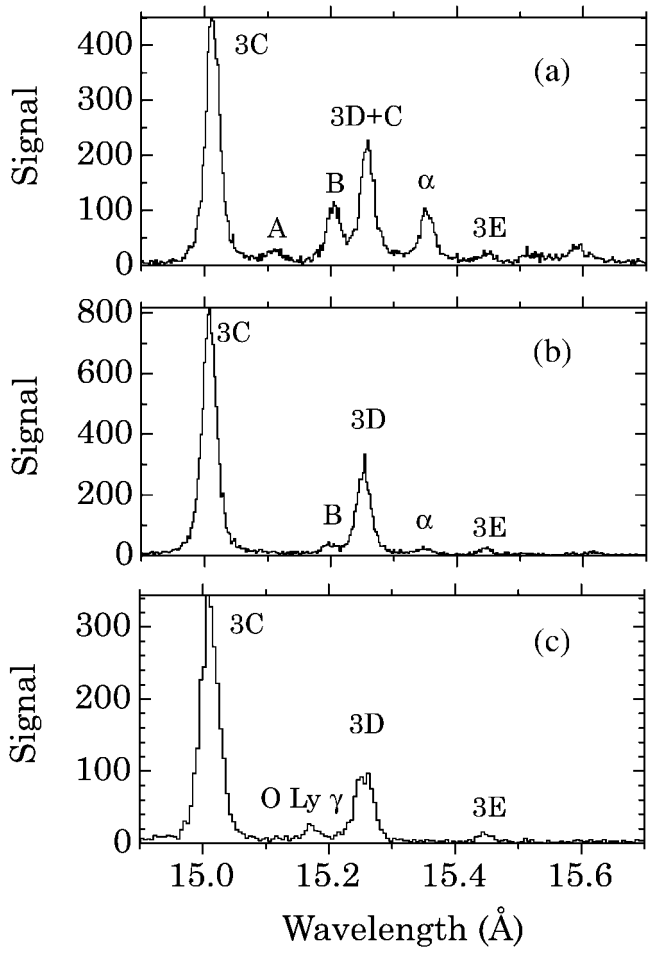

FIG. 1.—Fe L-shell spectra measured for different ionization balances: (*a*) very low ionization balance, high gas injector pressure; (*b*) low ionization balance, low gas injector pressure; (*c*) standard (equilibrium) ionization balance (typical for EBIT-II) obtained by iron injected with the MeVVA.

energetic electron beam set to 1140 ± 40 eV. The O VIII Lyγ line falls into the region of interest but is seen only in Figure 1*c*. Its absence in Figures 1*a* and 1*b* is surprising at first, given that five oxygen atoms are injected for each iron atom via the gas injector. The absence can be understood by the property of ion trapping in electron beam ion traps, where heavy ions are favored over light ions. The gas injector method offers an unlimited supply of heavy ions to fill the trap; the MeVVA method leaves room for lighter ions.

TABLE 1

RELATIVE INTENSITY OF THE LINE EMISSION FROM Fe XVI AND Fe XVII FOR THREE DIFFERENT CONDITIONS

Injection Condition (1)	R (2)	I_B/I_{3C} (3)	Fe XVI/Fe XVII (4)
High pressure	1.90 ± 0.11	0.339 ± 0.022	1.0
Low pressure	2.63 ± 0.15	0.0522 ± 0.0042	0.15
MeVVA injection	3.04 ± 0.12	0	0

NOTE.—Col. (4) shows the relative abundance of Fe XVI to Fe XVII inferred by using eq. (2); the relative line intensity of B and 3C is given in col. (3). All values have been corrected for foil transmission, crystal reflectivity, and polarization.

The wavelength scale was calibrated using the $3p \rightarrow 1s$ and $4p \rightarrow 1s$ lines in hydrogenic O VIII, whose wavelengths are given by Garcia & Mack (1965), and the lines 3C and 3D of neon-like Fe XVII, whose wavelengths are given by Brown et al. (1998).

Looking at Figure 1, we identify the IS satellites by inspection. We use the labels A, B, and α to mark the strongest of these. The intensities of A, B, and α decrease as the gas injector pressure, and thus, the abundance of lower charge states decreases. In Figure 1*c*, where the Fe XVII ion abundance is near 100%, the lines A, B, and α do not exist.

The ratios, R, from the spectra in Figure 1 are given in Table 1; R is much lower for the high-pressure case than in the low-pressure case. These ratios are corrected for foil transmission and crystal reflectivity. Also, because EBIT-II emits polarized radiation and the RAP crystals act as polarimeters, a correction for polarization is made (see below). The uncertainties in these ratios include the statistical uncertainty and the estimated uncertainty associated with the foil transmission and the crystal reflectivity.

Because there are no opacity effects on EBIT-II, and because at the electron beam energy of these measurements neither dielectronic recombination resonance nor resonance excitation may occur, these processes do not influence the spectra. Also, we have calculated the line emission from IS satellites of the Mg-like Fe XV ion in this wavelength band and find only one candidate, $1s^2 2s^2 2p^5_{1/2} 3s^2 3d_{3/2}\ J = 1 \rightarrow 1s^2 2s^2 2p^6 3s^2\ J = 0$, which we identify with line α.

The only process that can reduce R is a line coincidence of Na-like Fe XVI IS satellites with line 3D. To identify the coincident IS satellite, we considered the calculations of Zhang et al. (1989). The three Fe XVI IS transitions with the largest predicted excitation cross sections are given in Table 2. Note that the third line fully coincides with the location of 3D. We have also considered predictions by Cornille et al. (1994) and

TABLE 2

SUMMARY OF THE ATOMIC DATA COMPARED TO THE OBSERVED Fe XVI LINES

Label	Transition	λ^a (Å)	λ^b (Å)	σ^b ($\times 10^{-20}$ cm^2)	β^c	$P(90°)$	Relative Intensity[a]	Relative Intensity[d]
A	$2p_{1/2}3s3d_{3/2}\ J = 3/2 \rightarrow$ g.s.	15.115(6)	15.117	3.6	0.19	0.30	0.12	0.17
B	$2p_{1/2}3s3d_{3/2}\ J = 1/2 \rightarrow$ g.s.	15.208(4)	15.202	4.2	0.98	0.00	1	1
C	$2p_{1/2}3s3d_{5/2}\ J = 3/2 \rightarrow$ g.s.	15.26(2)[e]	15.263	4.6	0.46	0.23	0.55	0.51

NOTE.—"g.s." denotes the $1s^2 2s^2 2p^6 3s\ J = 1/2$ ground state of Fe XVI. The number in parentheses next to the measured wavelength is the uncertainty in the last digit.

[a] Present measurements.

[b] From Zhang et al. 1989.

[c] Present MCDF calculation.

[d] Present prediction.

[e] Blended with the Fe XVII 3D.

Phillips et al. (1997). These, however, leave out part of the atomic structure and are erroneous for the Fe XVI lines of interest here. Bautista (2000) corrected these problems but failed to resolve the relevant fine structure.

IS excited levels in Fe XVI can autoionize, and we therefore need to know the radiative branching ratios for each of these transitions before predicting the intensities. We must also know the polarization of each line. We calculated the radiative branching ratios using a multiconfigurational Dirac-Fock (MCDF) code (Chen 1985; Grant et al. 1980) and the polarization of each line using magnetic sublevel data from a distorted wave atomic code (Reed & Chen 1993; Zhang, Sampson, & Clark 1990). The polarization corrections make use of the ratio of the reflectivities of the parallel and perpendicular polarization components given by Henke, Gullikson, & Davis (1993)[3] for a mosaic crystal.

The relative intensity of the Na-like IS satellite lines predicted by our model and normalized to the well-resolved Fe XVI line B are given in Table 2. The relative intensity of line A agrees well with our measurements. The intensity of line C was deduced from the fact that R is 3.04 ± 0.12 when no blending occurs. Good agreement is found between the deduced and calculated value. The correction resulting from the polarization is only ~6% in the high-pressure case. Because the influence of the Fe XVI line is less in the low-pressure case and lines 3C and 3D have the same polarization, the polarization correction is ~2% in the low-pressure case. The correction from the foils and crystal reflectivity is ~4% for this line.

Recently, Laming et al. (2000) reported a laboratory measurement of 2.50 ± 0.13 for the 3C-to-3D ratio at 1.25 keV, which they claimed to be "more robust" than our earlier average value of 3.04 ± 0.12. In light of our present results and their significantly poorer resolution, we deem their claim erroneous and likely to be the result of spectral contamination

3. DISCUSSION

Because the apparent ratio R depends on line blending of Fe XVI IS satellites, we can write it as a function of the relative ion abundance, $n_{\rm Fe\,XVI}/n_{\rm Fe\,XVII}$; R is given by

$$R = \frac{I_{3C}}{I_{3D} + I_C} = \frac{\beta_{3C}\sigma_{3C}}{\beta_{3D}\sigma_{3D} + \beta_C\sigma_C(n_{\rm Fe\,XVI}/n_{\rm Fe\,XVII})}, \qquad (1)$$

where σ_{3C}, σ_{3D}, and σ_C are the total excitation cross sections and β_{3C}, β_{3D}, and β_C are the branching ratios. Using theoretical values for the cross sections given by Zhang et al. (1989) for the Na-like iron and Zhang & Sampson (1989) for Ne-like iron, and branching ratios given by our MCDF calculations, we plot R as a function of relative ion abundance (Fig. 2). The relative cross sections of the lines 3C to 3D has been set to 3.0 so that it agrees with the measured value given by Brown et al. (1998); i.e., we used Zhang's value of 1.18×10^{-19} cm^2 for the cross section of 3C, but 3.93×10^{-20} cm^2 for 3D rather than 3.13×10^{-20} cm^2 from Zhang. Future measurements are needed to give the actual cross sections.

By estimating the relative ion abundance from our measurements, we can plot the measured ratio as a function of relative ion abundance. We estimate the relative ion abundance during each of these measurements using the relative intensity

[3] Data from this work can be found at http://www-cxro.lbl.gov.

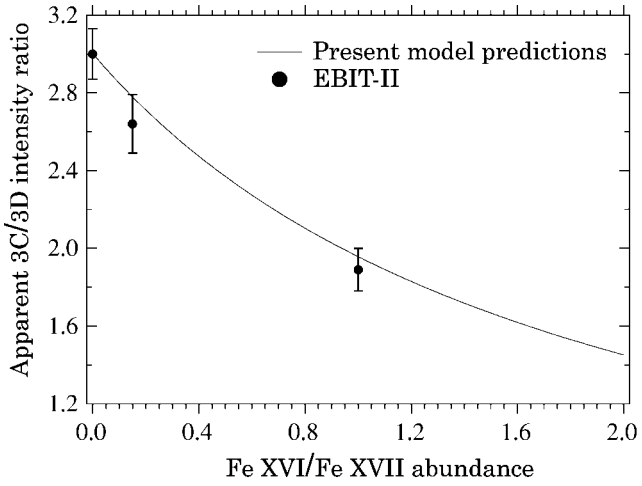

FIG. 2.—Ratio $R = I_{3C}/(I_{3D} + I_C)$ plotted as a function of Fe XVI/Fe XVII abundance. The solid curve is generated using eq. (1) with a relative cross section of lines 3C and 3D equal to 3.0.

of the Na-like line B to the Ne-like line 3C; i.e.,

$$\frac{n_{\rm Fe\,XVI}}{n_{\rm Fe\,XVII}} = \frac{I_B}{I_{3C}}\frac{\beta_{3C}\sigma_{3C}}{\beta_B\sigma_B}, \qquad (2)$$

where I_B/I_{3C} is the measured ratio corrected for spectrometer response. We use the theory of Zhang et al. (1989) and Zhang & Sampson (1989) to derive the relative ion abundance for each of the measured ratios given in Table 1. The measured values of R are plotted versus relative ion abundance in Figure 2. Because the derived relative abundances depend explicitly on the calculated excitation cross sections, using the results of other theories may change the derived relative abundance (≤30%).

Because R depends on the relative abundance of Fe XVI to Fe XVII, it can be used as a temperature diagnostic. Using the tables of Arnaud & Raymond (1992) to connect the relative ion abundance to the electron temperature, we plot R as a function of temperature in Figure 3. The diagnostic utility of this ratio covers the ~1–7 MK region where Arnaud & Raymond (1992) predict the Fe XVI–to–Fe XVII abundance to vary from 0.1 to 2.

The excitation cross sections for all lines vary as a function of electron impact energy. According to Zhang et al. (1989), the relative excitation cross section of line 3D to C increases by 10% and the relative intensity of line 3C to line B increases by approximately 10% from threshold to about 1.5 times threshold. This is a rather small variation and has little effect on the diagnostic utility of this ratio because in the low-temperature plasmas that contain a significant amount of Fe XVI, the line emission is determined by the cross section near threshold. This means that the curves shown in Figures 2 and 3 are valid in thermal plasmas within the 10%–30% accuracy of the collisional excitation calculations.

Using the curve in Figure 3, it is now possible to use R to determine the temperature of the solar corona and of extrasolar sources. In Figure 3, we plot previous measurements of R from flaring and nonflaring active regions of the Sun and the corona of Capella. The ratios and inferred temperatures from Figure 3 are given in Table 3. The temperatures that we determined for the solar active regions are consistent with the fact that the lower ratios were measured from cooler, nonflaring active regions, and

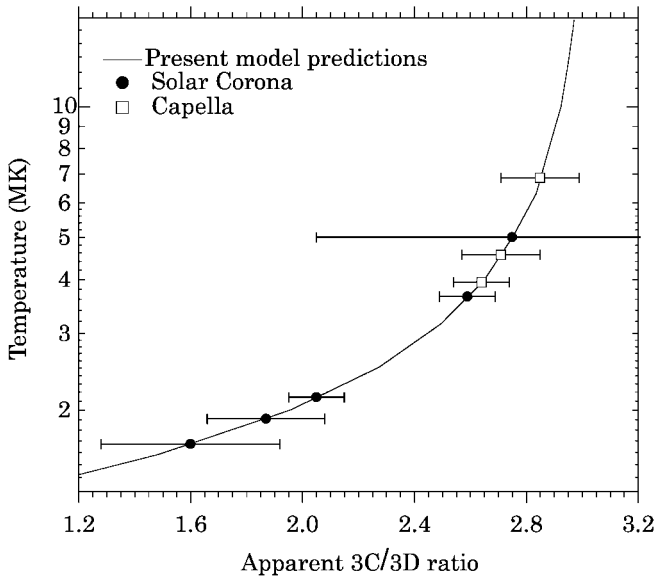

FIG. 3.—Correlation of the apparent 3C-to-3D ratio with the electron temperature. This curve is based on the relative ion abundance dependence of *R* given in Fig. 2 and the ion balance calculations of Arnaud & Raymond (1992). Observational points of the 3C-to-3D ratio are given in Table 3.

TABLE 3

TEMPERATURES DERIVED FROM FIGURE 3 FOR RATIOS, *R*, MEASURED IN THE CORONA OF THE SUN AND CAPELLA

Source	*R*	Temperature (MK)	References
Solar nonflaring active region	1.60 ± 0.32	1.67 ± 0.2	1
	1.87 ± 0.21	1.91 ± 0.2	2
	2.05 ± 0.1	2.14 ± 0.2	3
Solar flaring active region	2.59 ± 0.1	3.65 ± 0.5	4
	2.75 ± 0.7	5.00 ± 3	5
Capella	2.64 ± 0.10	3.94 ± 0.5	6[a]
	2.71 ± 0.14	4.56 ± 0.5	7[b]
	2.85 ± 0.14	6.85 ± 3	8[a]

[a] *Chandra* Low-Energy Transmission Grating Spectrometer.
[b] *Chandra* High-Energy Transmission Grating Spectrometer.
REFERENCES.—(1) Blake et al. 1965; (2) Waljeski et al. 1994; (3) Parkinson 1975; (4) Hutcheon et al. 1976; (5) McKenzie et al. 1980; (6) Brinkman et al. 2000; (7) Canizares et al. 2000; (8) Mewe et al. 2001.

the higher ratios are from hotter, flaring active regions. In the case of the Capella ratios, we deduce a temperature ranging from ~4 to 7 MK. These temperatures are consistent with those derived from helium-like and hydrogen-like line ratios from *Chandra* (Canizares et al. 2000; Brinkman et al. 2000), with the emission measure distribution derived from observations by *XMM-Newton* (Audard et al. 2001) and from *ASCA* and *Extreme Ultraviolet Explorer* spectra (Brickhouse et al. 2000).

In conclusion, we have shown that anomalously low 3C-to-3D ratios can be produced by a line coincidence with the $2p^5_{1/2}3s3d_{5/2}\ J = 3/2 \rightarrow 2p^6 3s\ J = 1/2$ Na-like Fe XVI IS satellite transition at 15.26 Å. While opacity effects may play a role in some plasmas, the ratio *R* should be used to infer such effects only after blending has been taken into account. As we showed, the solar and Capella observations can be fully explained by line blending at temperatures consistent with those inferred from other diagnostics without invoking opacity effects. Similarly, line blending is the only mechanism to explain tokamak observations that yielded an average value $R = 2.5$ (Beiersdorfer et al. 2001). If opacity effects are not an issue, *R* can be used to determine electron temperature from the inferred balance of Fe XVI and Fe XVII ions.

We acknowledge the dedicated technical support by E. Magee and P. D'Antonio. We thank D. Thorn for help in acquiring the data and B. Wargelin and R. Goddard at the Center for Astrophysics for providing us with the detector window. Work by the University of California, LLNL, was performed under contract W-7405-Eng-48 and supported by NASA SARA P.O. S-03958G and Smithsonian-*CXO* award EL9-1015A.

REFERENCES

Arnaud, M., & Raymond, J. 1992, ApJ, 398, 394
Audard, M., et al. 2001, A&A, 365, L329
Bautista, M. A. 2000, J. Phys. B, 33, 71
Beiersdorfer, P., et al. 2000a, in Atomic Data Needs for X-Ray Astronomy, ed. M. A. Bautista, T. R. Kallman, & A. K. Pradhan (Greenbelt: NASA/GSFC), 103
———. 2000b, Rev. Mexicana Astron. Astrofis. Ser. Conf., 9, 123
Beiersdorfer, P., von Goeler, S., Bitter, M., & Thorn, D. B. 2001, Phys. Rev. A, in press
Blake, R. L., Chubb, T. A., Friedman, H., & Unizicker, A. E. 1965, ApJ, 142, 1
Brickhouse, N. S., et al. 2000, ApJ, 530, 387
Brinkman, A. C., et al. 2000, ApJ, 530, L111
Brown, G. V. 2000, Ph.D. thesis, Auburn Univ.
Brown, G. V., Beiersdorfer, P., Kahn, S. M., Liedahl, D. A., & Widmann, K. 1998, ApJ, 502, 1015
Brown, G. V., Beiersdorfer, P., & Widmann, K. 1999, Rev. Sci. Instrum., 70, 280
———. 2001, Phys. Rev. A, 63, 032719
Canizares, C. R., et al. 2000, ApJ, 539, L41
Chen, M. H. 1985, Phys. Rev. A, 31, 1449
Cornille, M., Dubau, J., Faucher, P., Bely-Dubau, F., & Blanchard, C. 1994, A&AS, 105, 77
Garcia, J. D., & Mack, J. E. 1965, J. Opt. Soc. Am., 55, 654
Grant, I., McKenzie, B., Norrington, P., Mayers, D., & Pyper, N. 1980, Comput. Phys. Commun., 21, 207
Gu, M. F., et al. 1999, ApJ, 518, 1002
Henke, B. L., Gullikson, E. M., & Davis, J. C. 1993, At. Data Nucl. Data Tables, 54, 181
Hutcheon, R. H., Pye, F. P., & Evans, K. D. 1976, MNRAS, 175, 489
Laming, M., et al. 2000, ApJ, 545, L161
McKenzie, D. L., et al. 1980, ApJ, 241, 409
Mewe, R., et al. 2001, A&A, 368, 888
Parkinson, J. H. 1975, Sol. Phys., 42, 183
Phillips, K. J. H., et al. 1997, A&A, 324, 381
———. 1982, ApJ, 256, 774
Reed, K., & Chen, M. 1993, Phys. Rev. A, 48, 3644
Rugge, H. R., & McKenzie, D. L. 1985, ApJ, 297, 338
Saba, J. L. R., Schmelz, J. T., Bhatia, A. K., & Strong, K. T. 1999, ApJ, 510, 1064
Savin, D. W., et al. 1996, ApJ, 470, L73
Schmelz, J. T., Saba, J. L. R., Chauvin, J. C., & Strong, K. T. 1997, ApJ, 477, 509
Waljeski, K., et al. 1994, ApJ, 429, 909
Zhang, H. L., & Sampson, D. H. 1989, At. Data Nucl. Data Tables, 43, 1
Zhang, H. L., Sampson, D. H., & Clark, R. 1990, Phys. Rev. A, 41, 198
Zhang, H. L., Sampson, D. H., Clark, R. E. H., & Mann, J. B. 1989, At. Data Nucl. Data Tables, 41, 1